AGU100 ADVANCING EARTH AND SPACE SCIENCE

Geophysical Research Letters

RESEARCH LETTER
10.1029/2019GL083909

Voyager 2 constraints on plasmoid-based transport at Uranus

Gina A. DiBraccio[1] and Daniel J. Gershman[1]

[1]NASA Goddard Space Flight Center, Greenbelt, MD, USA

Key Points:
- Observations of a tailward moving plasmoid confirm that magnetotail reconnection contributes to magnetic flux circulation at Uranus
- The plasmoid's loop-like structure, with a decrease in field magnitude, suggests that internal forces play a role in mass transport
- Estimates indicate that plasmoids may serve as a major transport mechanism for mass loss through the Uranus magnetotail

Correspondence to:
G. A. DiBraccio,
gina.a.dibraccio@nasa.gov

Citation:
DiBraccio, G. A., & Gershman, D. J. (2019). Voyager 2 Constraints on Plasmoid-Based Transport at Uranus. *Geophysical Research Letters*, *46*, 10,710–10,718. https://doi.org/10.1029/2019GL083909

Received 28 MAY 2019
Accepted 7 AUG 2019
Accepted article online 09 AUG 2019
Published online 11 OCT 2019

Abstract A magnetosphere controls a planet's evolution by suppressing or enhancing atmospheric loss to space. In situ measurements of Uranus' magnetosphere from the Voyager 2 flyby in 1986 provide the only direct evidence of magnetospheric transport processes responsible for this atmospheric escape at Uranus. Analysis of high-resolution Voyager 2 magnetic field data in Uranus' magnetotail reveals the presence of a loop-like plasmoid filled with planetary plasma traveling away from the planet. This first plasmoid observation in an Ice Giant magnetosphere elucidates that (1) both internal and external forces play a role in Uranus' magnetospheric dynamics, (2) magnetic reconnection contributes to the circulation of plasma and magnetic flux at Uranus, and (3) plasmoids may be a dominant transport mechanism for mass loss through Uranus' magnetotail.

Plain Language Summary Uranus possesses an intrinsic magnetic field that encircles the planet and influences the local space environment. The solar wind plasma, made up of charged particles, flows away from the Sun and interacts with Uranus' magnetic field to form what is called a "planetary magnetosphere." By understanding dynamics of the magnetosphere, we are able to learn how changes in the Sun can impact the planet's space environment but also how magnetic fields and plasma are circulated throughout the system. In this work, we analyze data from the Voyager 2 spacecraft during the Uranus flyby in 1986. The data revealed a helical bundle of magnetic flux containing planetary plasma, known as a "plasmoid," in the tail of the magnetosphere. This first observation of a plasmoid in an Ice Giant magnetosphere elucidates processes that occur in the magnetosphere of Uranus and suggests that plasmoids may play a large role in transporting plasma.

1. Introduction

A planetary magnetosphere is formed as the high-speed solar wind plasma emanates from the Sun and interacts with a planet's intrinsic magnetic field. Magnetospheres influence a planet's evolution by regulating the circulation and removal of charged particles and magnetic flux within its local space environment. This removal of plasma, in the form of atmospheric loss to space, is an active area of research at planets throughout the solar system (see Catling & Kasting, 2017, and references therein). One conduit playing a significant role in this escape is "plasmoids," which are cylindrical bundles of magnetic flux filled with plasma (Hones, 1979). Plasmoids form as magnetic fields are "pinched off" in a planet's elongated magnetic tail by the plasma process of magnetic reconnection (Figure 1). These magnetic structures have been frequently observed in terrestrial intrinsic magnetospheres such as Mercury (DiBraccio, Slavin, et al., 2015; Slavin et al., 2009, 2010, 2012) and Earth (e.g., Hones, 1979; Hones, Baker, et al., 1984; Hones, Birn, et al., 1984; Ieda et al., 1998; Moldwin & Hughes, 1992; Slavin et al., 1989, 1993), the induced magnetosphere of Mars (Brain et al., 2010; DiBraccio, Espley, et al., 2015; Eastwood et al., 2008, 2012; Hara et al., 2017), and the Gas Giant magnetospheres of Jupiter (Kronberg et al., 2005, 2007, 2008; Vogt et al., 2010, 2014) and Saturn (Hill et al., 2008; Jackman et al., 2007, 2008, 2011, 2014, 2016). To date, no plasmoid observations have been reported from either of the Ice Giant magnetospheres: Uranus or Neptune. Here we utilize Voyager 2 data to confirm the presence of plasmoid-based mass loss and flux transport at Uranus.

At a distance of 19 AU from the Sun, Uranus experiences a limited degree of solar wind forcing. Typical upstream plasma densities of ~0.02 cm^{-3} and interplanetary magnetic field magnitudes of ~0.3 nT are low compared to values of ~7 cm^{-3} and ~8 nT at Earth (see Bagenal, 2013). While most planetary rotation axes are nearly perpendicular to the planet's orbital motion with respect to the Sun, Uranus' rotation axis is almost parallel, with a tilt of ~98°. For this reason, the angle between the solar wind and planetary

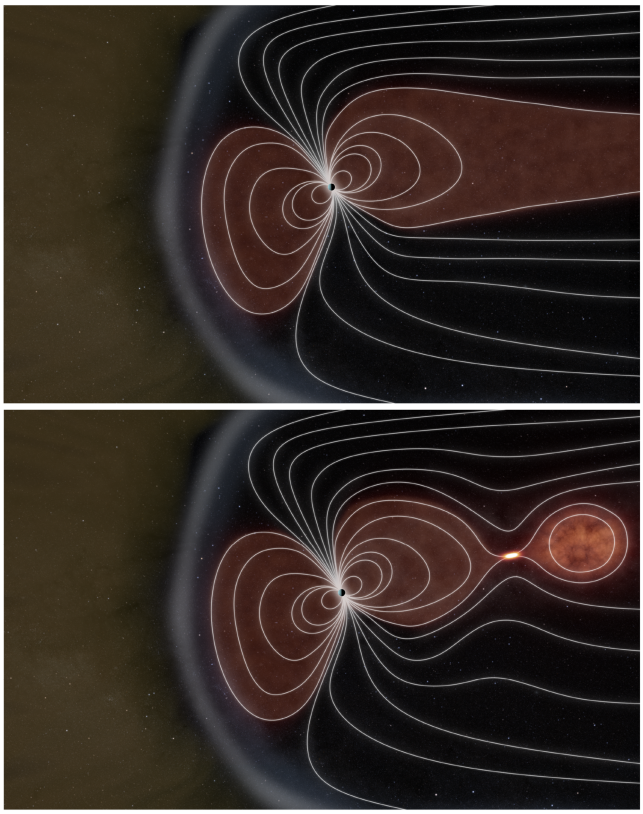

Figure 1. Graphic of the Uranus magnetosphere in a (top) quiescent and (bottom) active state, demonstrating the formation of a plasmoid in the magnetotail as a result of magnetic reconnection. The solar wind flows from the left to the right and the magnetosphere configuration is representative of the planet's orientation at the time of the Voyager 2 flyby.

rotation axis varies between 8° and 172° over the course of a Uranus year (84 Earth years). Furthermore, its planetary magnetic field is tilted ~59° from the rotation axis and shifted by 0.3 R_U (R_U is the radius of Uranus or 25,600 km) from the center of the planet (Connerney et al., 1987; Ness et al., 1986). This unusual geometry (Figure 1) generates tremendous diurnal and seasonal variations unlike any other planetary magnetosphere in the solar system (Cao & Paty, 2017; Masters, 2014).

Internal to the magnetosphere, the atmosphere of Uranus serves as a modest plasma source with protons acting as the dominant species at a production rate of ~0.02 kg/s (Bagenal, 2013; McNutt et al., 1987; Selesnick & McNutt, 1987). This relatively weak internal plasma source distinguishes Uranus from Jupiter and Saturn, whose magnetospheric mass contents are orders of magnitude higher due to the presence of active moons like Io (e.g., Delamere & Bagenal, 2003; Hill et al., 1983; Kivelson et al., 2004; Thomas et al., 2004) and Enceladus (e.g., Dougherty et al., 2006; Porco et al., 2006; Spencer et al., 2006). Nevertheless, in order to achieve a balanced system, planetary plasma mass loss processes at Uranus must account for its ~0.02 kg/s production rate.

The dynamics of a planetary magnetosphere and its plasmoid ejection processes leading to mass loss are preferentially driven by either external (i.e., solar wind) or internal (i.e., planetary rotation) forces; however, they may also exhibit a combination of the two. Earth and Mercury provide an example of externally driven environments, where the solar wind functions as the main magnetospheric source of both plasma and energy input. The giant magnetospheres of Jupiter and Saturn are dominated by internal dynamics due to the energy contributed by the planet's fast rotation, coupled with strong internal plasma sources and weak solar wind forcing (Khurana et al., 2004). Uranus' location in the heliosphere experiences an even weaker solar wind influence; however, Vasyliunas (1986) suggested that its magnetosphere can be externally dominated when there is close alignment between its rotation axis and the solar wind flow. Despite its distinctive nature, there is a dearth of in situ observations at Uranus, with only a single flyby of the Voyager 2 spacecraft in January 1986 (Stone & Miner, 1986). Therefore, the forces responsible for plasma transport and magnetospheric convection remain an outstanding question.

Here we report on the first observation of a plasmoid in the magnetotail of Uranus during the Voyager 2 flyby. This tailward moving plasmoid provides direct evidence that magnetic reconnection contributes to the circulation of magnetic flux and mass transport in the Ice Giant magnetospheres. Moreover, these observations offer new insights as to whether Uranus has an externally driven (i.e., solar wind) or internally driven (i.e., planetary rotation) magnetosphere. These single-point in situ measurements were analyzed to provide the first estimates of downtail plasma mass loss in an Ice Giant magnetosphere and the results are compared to analogous rates at the Gas Giants.

2. Analysis and Results

We revisit Voyager 2 Magnetometer (MAG) data (Behannon et al., 1977) obtained during the Uranus magnetotail transit. Previous studies of Uranus' magnetotail analyzed magnetic field vectors that were averaged over 48 s to several minutes in order to investigate large-scale structures. In this work, the analysis of MAG vectors at a finer resolution of 1.92 s revealed that a plasmoid was observed subsequent to the last complete cross-tail current sheet traversal (see "N3" in Behannon et al. (1987)). MAG data are presented in Uranus Solar Magnetospheric (USM) coordinates, equivalent to the Solar Magnetospheric (SM) coordinate system used in previous analyses of Voyager 2 data (e.g., Kane et al., 1991; Ness et al., 1986). In the USM coordinate system X_{USM} is directed toward the Sun along the Uranus-Sun line, Z_{USM} lies in the plane containing the X_{USM} axis and the magnetic dipole vector, and Y_{USM} completes the orthogonal, right-handed coordinate

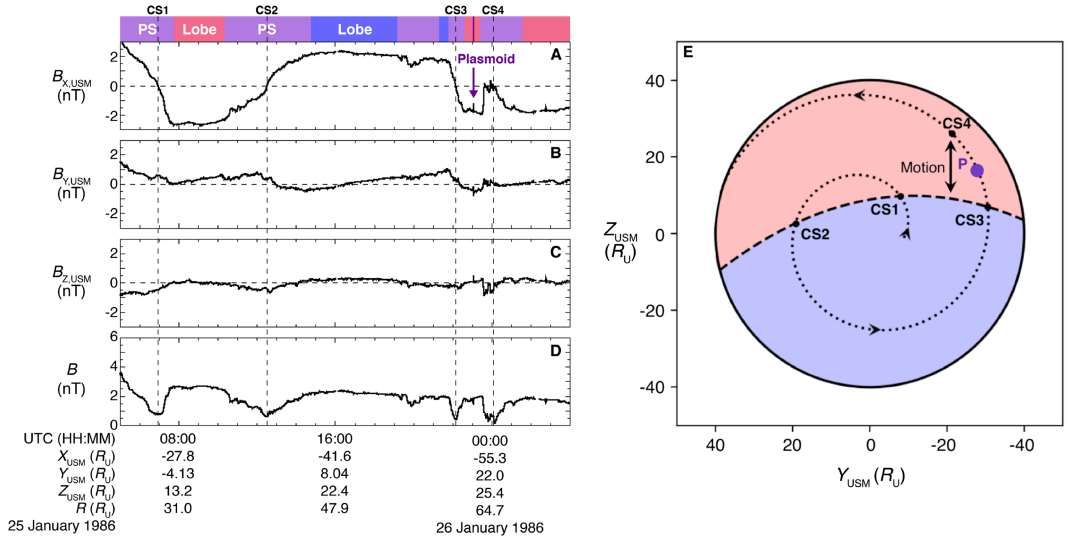

Figure 2. (a–d) Voyager 2 magnetic field data during the Uranus magnetotail traversal in USM coordinates. Four current sheet crossings (CS1–4), identified by Behannon et al. (1987), are indicated by vertical dashed lines. Regions shaded purple, red, and blue represent the plasma sheet (PS), $-B_{X,USM}$ tail lobe, and $+B_{X,USM}$ tail lobe, respectively. The observed plasmoid is labeled with a purple arrow. (e) A view of Uranus' magnetotail as seen from the tail looking toward the planet. The $-B_{X,USM}$ and $+B_{X,USM}$ lobes are represented by the red- and blue-shaded regions, respectively. The thick dashed line denotes the average plasma sheet location using a polynomial fit to the three complete current sheet crossings reported by Behannon et al. (1987). The dotted line shows Voyager 2's trajectory in the tail from the magnetospheric reference frame with the arrows indicating the spacecraft's progression. CS1–4 are labeled along the trajectory. The purple circle labeled "P" marks the spacecraft location at the time of the plasmoid observation.

system. Unfortunately, Uranus flyby data from the Voyager 2 Plasma Science (PLS) experiment are not available in the Planetary Data System beyond 25 January 1986 08:00 UTC, which is prior to the time period analyzed here. Therefore, we must rely on the published results by Sittler et al. (1987) and Behannon et al. (1987) for plasma parameters during the Uranus magnetotail traversal.

During the Uranus flyby, Voyager 2 first crossed the dayside magnetopause and entered the magnetosphere, it then encountered the planet at a closest approach of ~4.2 R_U, and finally traversed the magnetotail before exiting the magnetosphere ~45 hr later (Ness et al., 1986). The spacecraft measured the magnetotail out to a radial distance of ~79 R_U, providing measurements of the cross-tail current sheet and both magnetic tail lobes (Behannon et al., 1987). Multiple current sheet crossings were observed, indicating that this period was associated with significant magnetospheric activity and current sheet motion (Cheng et al., 1987; Mauk et al., 1987; McNutt et al., 1987).

Voyager 2 magnetic field observations of the Uranus magnetotail are displayed in Figures 2a–2d, spanning from 25 January 1986 05:00 UTC to 26 January 1986 04:00 UTC. This period included three complete and one partial current sheet crossings (CS1–4), identified as a change in $B_{X,USM}$ polarity and an incomplete $B_{X,MSO}$ rotation, respectively. The spacecraft observed both magnetic tail lobes and had multiple current sheet encounters due to both tail twisting effects caused by planetary rotation and current sheet dynamics (Behannon et al., 1987). The total field magnitude was ~2 nT in the lobes and decreased to ~0.5 nT in the central plasma sheet, encompassing the tail current sheet. A detailed overview and analysis of this magnetotail traversal is included in Behannon et al. (1987).

A loop-like plasmoid was observed between the third and fourth current sheet crossings (CS3 and CS4) at ~23:05 UTC on 25 January 1986 (Figure 2a). Voyager 2's location at the time of the plasmoid encounter is illustrated in Figure 2e. This tail view demonstrates that the structure was observed in the $-Y_{USM}$, $+Z_{USM}$ quadrant of the $-B_{X,USM}$ lobe (red region). The key magnetic field signatures used to classify this loop-like plasmoid were (1) a bipolar signature, representing an outer loop-like structure and (2) a local minimum in the field magnitude at the inflection point of the bipolar signature, suggesting the presence of trapped plasma. The significant rotation of the field observed throughout this structure distinguishes it from

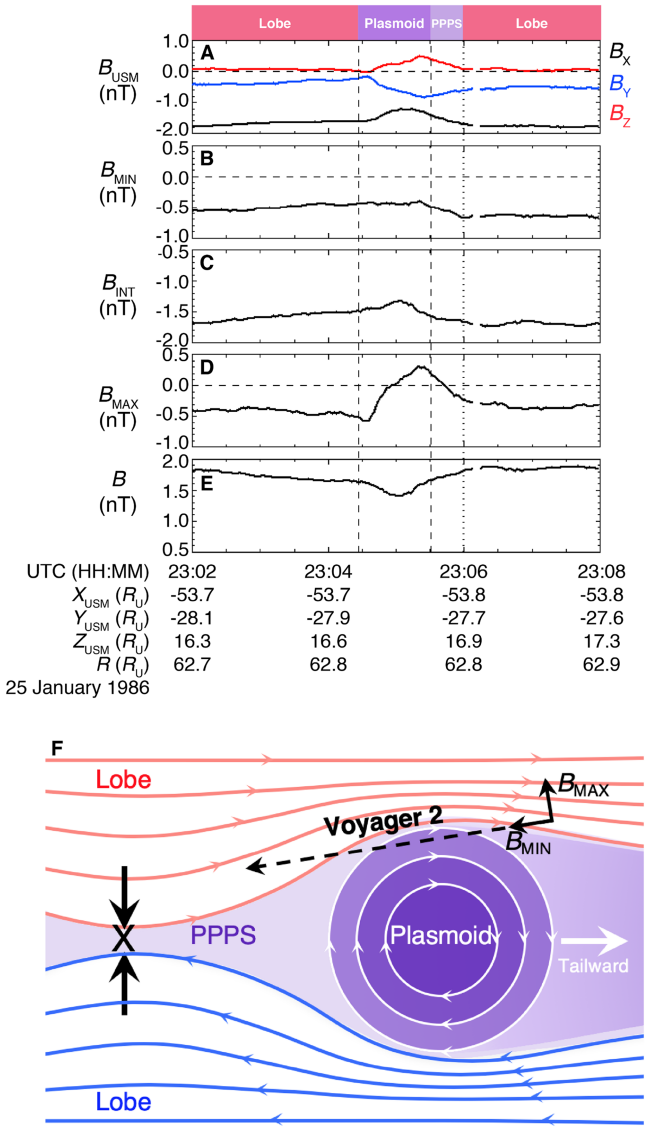

Figure 3. (a–e) Voyager 2 magnetic field data during the plasmoid encounter shown in (a) USM coordinates and (b–d) minimum variance analysis coordinates. The vertical dashed lines mark the plasmoid signature and are implemented for the minimum variance analysis interval. The postplasmoid plasma sheet (PPPS) is denoted as the region between end of the plasmoid (second vertical dashed line) and the vertical dotted line. (f) Schematic showing the Voyager 2 trajectory through the plasmoid and PPPS in Uranus' magnetotail as suggested by magnetic field signatures. Red and blue field lines represent the $-B_{X,USM}$ and $+B_{X,USM}$ tail lobes, respectively. The purple shaded region illustrates the central plasma sheet. The vertical black arrows indicate the open field line motion towards the current sheet with an "X" marking the location of the reconnection X-line. The horizontal white arrow demonstrates the tailward direction of the plasmoid after it has been ejected via magnetic reconnection.

neighboring partial crossings of the neutral sheet. The local minimum was likely associated with an increase in plasma pressure in order to maintain pressure balance (e.g., Hones, Baker, et al., 1984; Hones, Birn, et al., 1984; Jackman et al., 2014, 2016; Moldwin & Hughes, 1992; Vogt et al., 2010, 2014). This minimum in field magnitude also marks the differentiation between a loop-like plasmoid and a flux-rope plasmoid, which has a strong axially aligned core field that is observed as a local maxima in the magnetic field magnitude (e.g., Moldwin & Hughes, 1991; Sibeck et al., 1984; Slavin et al., 1995).

The plasmoid was observed for ~60 s at a downtail distance of ~54 R_U. In USM coordinates (Figure 3a), the plasmoid observations included bipolar signatures in $B_{Y,USM}$ and $B_{Z,USM}$ as the field rotated from ~−0.2 to ~−0.8 and ~0 to ~0.5 nT in these components, respectively. Given the orientation of the background planetary magnetic field at the time of the Voyager 2 encounter (Figures 2a–2d), a $B_{Z,USM}$ bipolar signature rotating from near-zero to the $+B_{Z,USM}$ lobe revealed that (1) the structure was moving tailward with a south-then-north signature and (2) the spacecraft encountered the edge of the plasmoid, away from the its central axis. The latter conclusion, of an off-axis crossing, is further supported by the fact that plasmoid signature was observed between a complete and partial current sheet crossing. If Voyager 2 measured the center of the plasmoid, the magnetic signatures would have been closer to, or embedded within, the current sheet and the $B_{Z,USM}$ signature would have crossed through zero.

The inflection points of the $B_{Y,USM}$ and $B_{Z,USM}$ bipolar signatures were aligned with a local minimum in $B_{X,USM}$ and B at the time of closest approach to the plasmoid center. Prior to entering the plasmoid, the magnitude of the background field in the magnetotail lobe was ~1.8 nT. This decreased down to ~1.4 nT within the plasmoid structure, before returning to its original lobe-field magnitude. Following the plasmoid encounter, the spacecraft observed an extended interval of $+B_{Z,USM}$ as the field recovered to its background state of $B_{Z,USM}$~0 at 23:06 UTC on 25 January 1986 (vertical dotted line Figures 3a–3e). This signature was identified as the postplasmoid plasma sheet (PPPS), a region where open fields in the tail lobes continued to undergo reconnection following the plasmoid formation and downtail ejection (Richardson et al., 1987; Richardson & Cowley, 1985). The duration of the PPPS was observed to be ~30 s. Figure 3f provides an illustration of the plasmoid and PPPS encounter in the magnetotail of Uranus.

To further assess the structure of this plasmoid, we applied a minimum variance analysis (Sonnerup & Cahill, 1967; Sonnerup & Scheible, 1998) over the period denoted by the vertical dashed lines in Figures 3a–3e. This interval was selected on the basis of the local maxima in the bipolar signatures of $B_{Y,USM}$ and $B_{Z,USM}$, consistent with analogous studies performed at Mercury, Jupiter, and Saturn (DiBraccio, Slavin, et al., 2015; Jackman et al., 2014; Vogt et al., 2014). The eigenvectors defining the minimum, intermediate, and maximum field variance directions were B_{MIN} = (0.20, 0.65, 0.74), B_{INT} = (0.88, 0.21, −0.42), and B_{MAX} = (0.42, −0.73, 0.53). The resulting intermediate-to-minimum and maximum-to-intermediate eigenvalue ratios were 16.9 and 19.6, respectively, which demonstrated that this coordinate system was well defined. Additionally, Behannon et al. (1987) found the Uranus current sheet to be curved out near the flanks relative to the Y_{USM}–Z_{USM} plane, which is consistent the B_{MAX} eigenvector defined here. Throughout the interval, B_{MIN} was nonzero and nearly constant at ~0.5 nT, further supporting that the spacecraft did not observe the

center of the structure. The local minimum measured during the spacecraft's closest approach to the plasmoid center was observed in B_{INT} and represented the axial direction of the plasmoid. This decrease in field magnitude indicated the presence of trapped plasma from the central plasma sheet in the loop-like structure of the plasmoid. In flux-rope-type plasmoids, a local maximum would have been observed along B_{INT}. Finally, the bipolar signature was clearly observed in B_{MAX} and rotated from −0.5 to +0.3 nT.

3. Discussion

The detection of plasmoids in a planetary magnetotail elucidates (1) the occurrence and frequency of magnetic reconnection, (2) the mechanisms responsible for plasma acceleration and mass loss, and (3) the overall dynamical processes that dominate a particular magnetosphere. The plasmoid observed in Uranus' magnetotail during the 1986 Voyager 2 flyby had a loop-like structure with a diamagnetic decrease, indicating the presence of trapped charged particles from the central plasma sheet. The identification of a plasmoid in this region provides direct evidence that atmospheric plasma was removed from the system and that magnetic reconnection was occurring in the cross-tail current sheet, as originally postulated by charged particle measurements (Mauk et al., 1987) and more recent numerical simulations (Tóth et al., 2004).

The location of the observed plasmoid at ~54 R_U downtail constrains the location of the tail reconnection X-line to be planetward of this distance. This finding supports simulation results reported by Tóth et al. (2004) where magnetic fields reconnected at downtail distances of ~30 R_U. Additionally, although not explicitly highlighted, magnetospheric dynamics simulations during Uranus' solstice season presented by Cao and Paty (2017) appear to have included a bundle of magnetic flux located ~50–60 R_U downtail in the simulation domain.

In order to quantify plasmoid-based transport at Uranus, estimates of the structure's size, content, and occurrence frequency are necessary. The use of single-point magnetic field observations to determine plasmoid scale sizes can result in significant uncertainties (e.g., DiBraccio, Slavin, et al., 2015; Jackman et al., 2014; Slavin et al., 1993; Vogt et al., 2014); however, these data help to provide quantitative constraints on plasmoid content. In order to develop the first constraints at Uranus, we apply an analytical approach that has been previously conducted on plasmoid observations at both Jupiter and Saturn (Jackman et al., 2014; Vogt et al., 2014). It is important to note that systematic biases introduced when estimating structure size with this technique should be similar across all giant planet systems (Cowley et al., 2015).

We use the local Alfvén speed as a proxy for plasmoid propagation in order to estimate the spatial scale of the plasmoid without the availability of plasma flow measurements. Within the central plasma sheet, the magnetic field magnitude was ~0.5 nT and the observed electron density was ~3×10^{-3} cm^{-3} (Sittler et al., 1987). In the tail lobes, the field strength was ~2 nT, with an electron density of ~1×10^{-3} cm^{-3} (Sittler et al., 1987). Assuming quasi-neutrality and that protons were the dominant ion species (Selesnick & McNutt, 1987), the local Alfvén speeds in the central plasma sheet and adjacent tail lobes were ~200 km/s and ~1,400 km/s, respectively. Because the observed plasmoid transport included contributions from both plasma sheet and lobe reconnection, as supported by PPPS observations, the structure speed was likely between these two limits (Slavin et al., 2003). Therefore, the ~60-s plasmoid duration determined by the bipolar signature peaks corresponded to length scales between ~0.5 R_U and 3.3 R_U. We adopt ~2 R_U as the average length scale.

When estimating the plasmoid length and height, we consider that Voyager 2 did not pass through the center of the structure and, therefore, determine that the average length of ~2 R_U is likely an underestimate. The force-free flux rope model of Kivelson and Khurana (1995) demonstrated that inferring plasmoid lengths from magnetic signatures can lead to systematic underestimates by a factor of ~4–8 (see Vogt et al. (2014) and Jackman et al. (2014) for the implementation of this assumption at the Gas Giants). Additionally, at Earth, it has been determined that the plasmoid height is roughly twice the plasma sheet thickness (Slavin et al., 1993). Behannon et al. (1987) reported an average plasma sheet thickness of ~10 R_U in the region where the plasmoid was observed in Uranus' magnetotail. Taking these factors into account, we suggest that the observed plasmoid was likely a cylindrical structure with a diameter between ~8 and ~16 R_U.

As with previous studies at Jupiter and Saturn, the plasmoid's azimuthal extent across the tail was not directly measurable. In the internally driven magnetospheres of Jupiter and Saturn, tail reconnection

may be constrained to ~10% of the tail width (Vogt et al., 2010, 2014), while at highly externally driven magnetospheres (e.g., Mercury), the full tail width is typically assumed for plasmoid flux calculations (DiBraccio, Slavin, et al., 2015). At Uranus, Ness et al. (1986) and Behannon et al. (1987) found the cross-tail width to be ~80 R_U. The plasmoid's azimuthal extent could therefore range from ~8 R_U to 80 R_U.

The presence of a PPPS indicated externally driven magnetic reconnection continued between the open fields in the tail lobes after the closed-field plasmoid was ejected. This continuation of reconnection removed open magnetic flux from the magnetotail, balancing its creation on the dayside via magnetopause reconnection (Dungey, 1961; Masters, 2014). The observed change in $B_{Z,USM}$ of ~0.32 nT over a duration of 30 s in the PPPS indicated that ~16 MWb of open tail magnetic flux was detached from the planet, assuming that the full tail width (80 R_U) was undergoing reconnection. Although this number is likely a lower estimate of flux given that the spacecraft observed the edge of the plasmoid and PPPS, it was nonetheless significantly small (i.e., <1%) compared to the ~3.3 GWb of flux contained in the tail lobe. Note that in the instance where reconnection is not occurring across the full tail width (i.e., <80 R_U), this result would be even less and it would require an extended period of open-field reconnection to cycle through the entire tail lobe flux. However, this minimal PPPS contribution of flux removal is comparable to calculations at Jupiter (Vogt et al., 2014).

With a wide range of potential plasmoid dimensions, we estimate its content by assuming a cylindrical structure and applying a Monte Carlo simulation that considers uniformly distributed, independent values in diameter (ranging from 8 R_U to 16 R_U) and azimuthal extent (ranging from 8 R_U to 80 R_U). This analysis results in a mean plasmoid volume of $8.7 \pm 5.4 \times 10^{31}$ cm^3, where the uncertainty is calculated as the standard deviation from the mean. For a plasma sheet density of ~3×10^{-3} cm^{-3}, this volume translates to a proton mass of ~430 $\pm$ 270 kg within the plasmoid.

By utilizing this mass content, we can apply an estimated occurrence rate to assess the plasmoid contribution to plasma transport at Uranus. It has been suggested that dayside reconnection occurs on the order of ~17 hr at Uranus. This frequency, reported by Richardson et al. (1988), was determined through observations of periodic velocity decreases in Uranus' flank magnetosheath that were associated with the planetary rotation. Given that the magnetotail rotates with the planet, we take 17 hr as a reference for the plasmoid ejection rate. The series of tail current sheet crossings observed by Voyager 2 at downtail distances exceeding ~30 R_U occurred over an ~15-hr interval, such that identification of a single plasmoid ejection in this period is consistent with the available spacecraft data. Therefore, using ~17 hr as the plasmoid occurrence frequency, we estimate a plasmoid-based mass loss rate of ~0.007 $\pm$ 0.004 kg/s at Uranus. This corresponds to ~35 $\pm$ 20% of the ~0.02 kg/s atmospheric proton production rate estimated by Bagenal (2013).

Plasmoids observed at Uranus, Jupiter, and Saturn have a similar loop-like topology, which is indicative of internal driving (Jackman et al., 2014; Vogt et al., 2014). Mass loss in the internally driven magnetospheres of Jupiter and Saturn are dominated by diffusive-based processes (e.g., Delamere et al., 2015; Kane et al., 2014; Kivelson & Southwood, 2005; Louarn et al., 2015), with plasmoid-based loss contributing to only ~5–15% of the total production rate when applying the same analytical methods as presented above (Jackman et al., 2014; Vogt et al., 2014). Because the conservative lower limit of the mass-loss calculation derived here is greater than corresponding estimates for Jupiter and Saturn, it is possible that plasmoid ejection may be a dominant mass-loss mechanism at Uranus.

It is surprising to observe a loop-like plasmoid in a magnetosphere that is not only expected to be externally dominated (Selesnick & Richardson, 1986; Vasyliunas, 1986) but, more importantly, one that also experiences a natural helical tail twist due to the planet's rotation axis orientation (Behannon et al., 1987; Voigt et al., 1987). Voyager 2 observations of a plasmoid in Uranus' magnetic tail reveal that we do not yet adequately understand the processes driving Ice Giant magnetospheres. With an ever-changing interaction between the solar wind and planetary magnetic field, Uranus presents a unique challenge for comparing external versus internal magnetospheric dynamics. Because these dynamics greatly influence atmospheric loss to space, identifying the forces driving a magnetosphere will lead to clues about the planet's evolution. From the analysis presented here, we are able to make the following points in order to advance our understanding of the forces responsible for plasma and flux transport within the Uranus system:

1. The presence of a tailward-moving plasmoid with trapped plasma confirms that magnetic reconnection contributes to the circulation of magnetic flux and removal of atmospheric plasma within a magnetosphere that exhibits large tilts in both the rotation and magnetic field axes.
2. The loop-like structure was not expected to be observed in a solar wind-driven magnetosphere with a twisted tail caused by the planetary rotation, suggesting that internal forces play a role in mass transport at Uranus.
3. Plasmoids may serve as a major transport mechanism for mass loss through the Uranus magnetotail.
4. The amount of open magnetic flux that is reconnected and released through the PPPS is likely sufficiently less than the total lobe flux, indicating that an externally dominated environment would require unrealistic timescales to release the total open flux.

Although no relevant measurements are available for Neptune due to the 1989 Voyager 2 flyby trajectory (Stone & Miner, 1989), we suggest that its systematic mass loss may include a significant plasmoid contribution as well. Similar to Uranus, Neptune's magnetosphere exhibits a large variance between the rotation and magnetic axes at an angle of ~47°. However, in contrast to Uranus, Neptune's rotation axis is not aligned with the solar wind (~30° inclination). This difference may allow for internal effects to play a larger role in mass loss and overall plasma convection. For this reason, unlike at other magnetospheres throughout the solar system, the planet's rotation and solar wind forcing may have nearly equal contributions to the energy and plasma input at Uranus and Neptune.

The nature of magnetospheric circulation and mass-loss processes remain outstanding and essential topics at both Uranus and Neptune. In order to definitively determine the relative contributions of planetary rotation and solar wind forcing in driving global plasma dynamics, new in situ measurements will be necessary. Until then, the enigmatic Ice Giant magnetospheres await further exploration.

Acknowledgments
The authors gratefully acknowledge internal support from the Solar System Exploration Division within the NASA Goddard Space Flight Center (GSFC) Sciences and Exploration Directorate. We sincerely appreciate the artistic skills of Walter Feimer and the NASA GSFC Conceptual Image Lab (http://cilab.gsfc.nasa.gov/) in developing the graphics in Figure 1. The authors thank the Voyager 2 team for providing high-quality archive data and for their initial analysis on the magnetotail of Uranus. Voyager 2 Magnetometer data are publicly available on the Planetary Plasma Interactions (PPI) Node of the Planetary Data System (PDS): https://pds-ppi.igpp.ucla.edu/mission/Voyager/VG2/MAG.

References

Bagenal, F. (2013). Planetary magnetospheres. In L. M. French, P. Kalas, & T. D. Oswalt (Eds.), *Planets, stars and stellar systems* (Chap. 6, Vol. 3, pp. 251–308). Dordrecht: Springer.

Behannon, K. W., Acuña, M. H., Burlaga, L. F., Lepping, R. P., Ness, N. F., & Neubauer, F. M. (1977). Magnetic field experiment for Voyagers 1 and 2. *Space Science Reviews*, *21*, 235–257.

Behannon, K. W., Lepping, R. P., Sittler, E. C. Jr., Ness, N. F., Mauk, B. H., Krimigis, S. M., & McNutt, R. L. Jr. (1987). The magnetotail of Uranus. *Journal of Geophysical Research*, *92*, 15,354–15,366.

Brain, D. A., Baker, A. H., Briggs, J., Eastwood, J. P., Halekas, J. S., & Phan, T.-D. (2010). Episodic detachment of Martian crustal magnetic fields leading to bulk atmospheric plasma escape. *Geophysical Research Letters*, *37*, L14108. https://doi.org/10.1029/2010GL043916

Cao, X., & Paty, C. (2017). Diurnal and seasonal variability of Uranus's magnetosphere. *Journal of Geophysical Research: Space Physics*, *122*, 6318–6331.

Catling, D., & Kasting, J. (2017). Escape of atmospheres to space. In *Atmospheric evolution on inhabited and lifeless worlds* (Chap. 5, pp. 129–168). Cambridge.

Cheng, A. F., Krimigis, S. M., Mauk, B. H., Keath, E. P., Maclennan, C. G., Lanzerotti, L. J., et al. (1987). Energetic ion and electron phase space densities in the magnetosphere of Uranus. *Journal of Geophysical Research*, *92*, 15,315–15,328.

Connerney, J. E. P., Acuña, M. H., & Ness, N. F. (1987). The magnetic field of Uranus. *Journal of Geophysical Research*, *92*(A13), 15,329–15,336. https://doi.org/10.1029/JA092iA13p15329

Cowley, S. W. H., Nichols, J. D., & Jackman, C. M. (2015). Down-tail mass loss by plasmoids in Jupiter's and Saturn's magnetospheres. *Journal of Geophysical Research: Space Physics*, *120*, 6347–6356.

Delamere, P., Bagenal, F., Paranicas, C., Masters, A., Radioti, A., Bonfond, B., et al. (2015). Solar wind and internally driven dynamics: Influences on magnetodiscs and auroral responses. *Space Science Reviews*, *187*(1-4), 51–97. https://doi.org/10.1007/s11214-014-0075-1

Delamere, P. A., & Bagenal, F. (2003). Modeling variability of plasma conditions in the Io torus. *Journal of Geophysical Research*, *108*(A7), 1276. https://doi.org/10.1029/2002JA009706

DiBraccio, G. A., Espley, J. R., Gruesbeck, J. R., Connerney, J. E. P., Brain, D. A., Halekas, J. S., et al. (2015). Magnetotail dynamics at Mars: Initial MAVEN observations. *Geophysical Research Letters*, *42*, 8828–8837. https://doi.org/10.1002/2015GL065248

DiBraccio, G. A., Slavin, J. A., Imber, S. M., Gershman, D. J., Raines, J. M., Jackman, C. M., et al. (2015). MESSENGER observations of flux ropes in Mercury's magnetotail. *Planetary and Space Science*, *115*, 77–89. https://doi.org/10.1016/j.pss.2014.12.016

Dougherty, M. K., Khurana, K. K., Neubauer, F. M., Russell, C. T., Saur, J., Leisner, J. S., & Burton, M. E. (2006). Identification of a dynamic atmosphere at Enceladus with the Cassini Magnetometer. *Science*, *311*(5766), 1406–1409. https://doi.org/10.1126/science.1120985

Dungey, J. W. (1961). Interplanetary magnetic field and the auroral zones. *Physical Review Letters*, *6*(2), 47–48. https://doi.org/10.1103/PhysRevLett.6.47

Eastwood, J. P., Brain, D. A., Halekas, J. S., Drake, J. F., Phan, T. D., Øieroset, M., et al. (2008). Evidence for collisionless magnetic reconnection at Mars. *Geophysical Research Letters*, *35*, L02106. https://doi.org/10.1029/2007GL032289

Eastwood, J. P., Videira, J. J. H., Brain, D. A., & Halekas, J. S. (2012). A chain of magnetic flux ropes in the magnetotail of Mars. *Geophysical Research Letters*, *39*, L03104. https://doi.org/10.1029/2011GL050444

Hara, T., Harada, Y., Mitchell, D. L., DiBraccio, G. A., Espley, J. R., Brain, D. A., et al. (2017). On the origins of magnetic flux ropes in near-Mars magnetotail current sheets. *Geophysical Research Letters*, *44*, 7653–7662. https://doi.org/10.1002/2017GL073754

Hill, T. W., Dessler, A. J., & Goertz, C. K. (1983). Magnetospheric models. In A. J. Dessler (Ed.), *Physics of the Jovian Magnetosphere* (pp. 353–394). https://doi.org/10.1017/CBO9780511564574.012

Hill, T. W., Thomsen, M. F., Henderson, M. G., Tokar, R. L., Coates, A. J., McAndrews, H. J., et al. (2008). Plasmoids in Saturn's magnetotail. *Journal of Geophysical Research*, *113*, A01214.
Hones, E. W. (1979). Transient phenomena in the magnetotail and their relation to substorms. *Space Science Reviews*, *23*, 393–410.
Hones, E. W., Baker, D. N., Bame, S. J., Feldman, W. C., Gosling, J. T., McComas, D. J., et al. (1984). Structure of the magnetotail at 220-Re and its response to geomagnetic-activity. *Geophysical Research Letters*, *11*(1), 5–7. https://doi.org/10.1029/GL011i001p00005
Hones, E. W., Birn, J., Baker, D. N., Bame, S. J., Feldman, W. C., McComas, D. J., et al. (1984). Detailed examination of a plasmoid in the distant magnetotail with Isee-3. *Geophysical Research Letters*, *11*(10), 1046–1049. https://doi.org/10.1029/GL011i010p01046
Ieda, A., Machida, A., Mukai, T., Saito, Y., Yamamoto, T., Nishida, A., et al. (1998). Statistical analysis of the plasmoid evolution with Geotail observations. *Journal of Geophysical Research*, *103*(A3), 4453–4465. https://doi.org/10.1029/97JA03240
Jackman, C. M., Arridge, C. S., Krupp, N., Bunce, E. J., Mitchell, D. G., McAndrews, H. J., et al. (2008). A multi-instrument view of tail reconnection at Saturn. *Journal of Geophysical Research*, *113*, A11213.
Jackman, C. M., Provan, G., & Cowley, S. W. H. (2016). Reconnection events in Saturn's magnetotail: Dependence of plasmoid occurrence on planetary period oscillation phase. *Journal of Geophysical Research: Space Physics*, *121*, 2922–2934.
Jackman, C. M., Russell, C. T., Southwood, D. J., Arridge, C. S., Achilleos, N., & Dougherty, M. K. (2007). Strong rapid dipolarizations in Saturn's magnetotail: In situ evidence of reconnection. *Geophysical Research Letters*, *34*, L11203. https://doi.org/10.1029/2007GL029764
Jackman, C. M., Slavin, J. A., & Cowley, S. W. H. (2011). Cassini observations of plasmoid structure and dynamics: Implications for the role of magnetic reconnection in magnetospheric circulation at Saturn. *Journal of Geophysical Research*, *116*, A10212.
Jackman, C. M., Slavin, J. A., Kivelson, M. G., Southwood, D. J., Achilleos, N., Thomsen, M. F., et al. (2014). Saturn's dynamic magnetotail: A comprehensive magnetic field and plasma survey of plasmoids and traveling compression regions and their role in global magnetospheric dynamics. *Journal of Geophysical Research: Space Physics*, *119*, 5465–5494.
Kane, M., Mauk, B. H., Keath, E. P., & Krimigis, S. M. (1991). Structure and dynamics of the Uranian magnetotail: Results from hot plasma and magnetic field observations. *Journal of Geophysical Research*, *96*, 11,485–11,499.
Kane, M., Mitchell, D. G., Carbary, J. F., & Krimigis, S. M. (2014). Plasma convection in the nightside magnetosphere of Saturn determined from energetic ion anisotropies. *Planetary and Space Science*, *91*, 1–13. https://doi.org/10.1016/j.pss.2013.10.001
Khurana, K. K., Kivelson, M. G., Vasyliunas, V. M., Krupp, N., Woch, J., Lagg, A., et al. (2004) ch. 24). The configuration of Jupiter's magnetosphere. In F. Bagenal, T. E. Dowling, & W. B. McKinnon (Eds.), *Jupiter: The planet, satellites and magnetosphere* (pp. 593–616). Cambridge: University Press.
Kivelson, M. G., Bagenal, F., Kurth, W. S., Neubauer, F. M., Paranicas, C., & Saur, J. (2004). *J Magnetospheric interactions with satellites Jupiter Book*. Cambridge: Cambridge University Press.
Kivelson, M. G., & Khurana, K. K. (1995). Models of flux ropes embedded in a Harris neutral sheet: Force-free solutions in low and high beta plasmas. *Journal of Geophysical Research*, *100*(A12), 23,637–23,645. https://doi.org/10.1029/95JA01548
Kivelson, M. G., & Southwood, D. J. (2005). Dynamical consequences of two modes of centrifugal instability in Jupiter's outer magnetosphere. *Journal of Geophysical Research*, *110*(A12), A12209. https://doi.org/10.1029/2005JA011176
Kronberg, E. A., Glassmeier, K.-H., Woch, J., Krupp, N., Lagg, A., & Dougherty, M. K. (2007). A possible intrinsic mechanism for the quasiperiodic dynamics of the Jovian magnetosphere. *Journal of Geophysical Research*, *112*, A05203.
Kronberg, E. A., Woch, J., Krupp, N., & Lagg, A. (2008). Mass release process in the Jovian magnetosphere: Statistics on particle burst parameters. *Journal of Geophysical Research*, *113*, A10202.
Kronberg, E. A., Woch, J., Krupp, N., Lagg, A., Khurana, K. K., & Glassmeier, K.-H. (2005). Mass release at Jupiter: Substorm-like processes in the Jovian magnetotail. *Journal of Geophysical Research*, *110*, A03211.
Louarn, P., Andre, N., Jackman, C. M., Kasahara, S., Kronberg, E. A., & Vogt, M. F. (2015). Magnetic reconnection and associated transient phenomena within the magnetospheres of Jupiter and Saturn. *Space Science Reviews*, *187*(1-4), 181–227. https://doi.org/10.1007/s11214-014-0047-5
Masters, A. (2014). Magnetic reconnection at Uranus' magnetopause. *Journal of Geophysical Research: Space Physics*, *119*, 5520–5538.
Mauk, B. H., Krimigis, S. M., Keath, E. P., Cheng, A. F., Armstrong, T. P., Lanzerotti, L. J., et al. (1987). The hot plasma and radiation environment of the Uranian magnetosphere. *Journal of Geophysical Research*, *92*(15), 283–15,308.
McNutt, R. L., Selesnick, R. S., & Richardson, J. D. (1987). Low-energy plasma observations in the magnetosphere of Uranus. *Journal of Geophysical Research*, *92*(A5), 4399–4410. https://doi.org/10.1029/JA092iA05p04399
Moldwin, M. B., & Hughes, W. J. (1991). Plasmoids as magnetic flux ropes. *Journal of Geophysical Research*, *96*, 14,051–14,064.
Moldwin, M. B., & Hughes, W. J. (1992). On the formation and evolution of plasmoids: A survey of ISEE 3 geotail data. *Journal of Geophysical Research*, *97*(A12), 19,259–19,282. https://doi.org/10.1029/92JA01598
Ness, N. F., Acuña, M. H., Behannon, K. W., Burlaga, L. F., Connerney, J. E. P., Lepping, R. P., & Neubauer, F. M. (1986). Magnetic fields at Uranus. *Science*, *233*(4759), 85–89. https://doi.org/10.1126/science.233.4759.85
Porco, C. C., Helfenstein, P., Thomas, P. C., Ingersoll, A. P., Wisdom, J., West, R., et al. (2006). Cassini observes the active south pole of Enceladus. *Science*, *311*(5766), 1393–1401. https://doi.org/10.1126/science.1123013
Richardson, I. G., & Cowley, S. W. H. (1985). Plasmoid-associated energetic ion bursts in the deep geomagnetic tail: Properties of the boundary layer. *Journal of Geophysical Research*, *90*(A12), 12,133–12,158. https://doi.org/10.1029/JA090iA12p12133
Richardson, I. G., Cowley, S. W. H., Hones, E. W., & Bame, S. J. (1987). Plasmoid-associated energetic ion bursts in the deep geomagnetic tail: Properties of plasmoids and the postplasmoid plasma sheet. *Journal of Geophysical Research*, *92*, 9,997–10,013.
Richardson, J. D., Belcher, J. W., Selesnick, R. S., Zhang, M., Siscoe, G. L., & Eviatar, A. (1988). Evidence for periodic reconnection at Uranus? *Geophysical Research Letters*, *15*(8), 733–736. https://doi.org/10.1029/GL015i008p00733
Selesnick, R. S., & McNutt, R. L. (1987). Voyager 2 plasma ion observations in the magnetosphere of Uranus. *Journal of Geophysical Research*, *92*(A13), 15,249–15,262. https://doi.org/10.1029/JA092iA13p15249
Selesnick, R. S., & Richardson, J. D. (1986). Plasmasphere formation in arbitrarily oriented magnetospheres. *Geophysical Research Letters*, *13*(7), 624–627. https://doi.org/10.1029/GL013i007p00624
Sibeck, D. G., Siscoe, G. L., Slavin, J. A., Smith, E. J., Bame, S. J., & Scarf, F. L. (1984). Magnetotail flux ropes. *Geophysical Research Letters*, *11*(10), 1090–1093. https://doi.org/10.1029/GL011i010p01090
Sittler, E. C., Ogilvie, K. W., & Selesnick, R. (1987). Survey of electrons in the Uranian magnetosphere: Voyager 2 observations. *Journal of Geophysical Research*, *92*(A13), 15,263–15,281. https://doi.org/10.1029/JA092iA13p15263
Slavin, J. A., Acuña, M. H., Anderson, B. J., Baker, D. N., Benna, M., Boardsen, S. A., et al. (2009). MESSENGER observations of magnetic reconnection in Mercury's magnetosphere. *Science*, *324*(5927), 606–610. https://doi.org/10.1126/science.1172011
Slavin, J. A., Anderson, B. J., Baker, D. N., Benna, M., Boardsen, S. A., Gloeckler, G., et al. (2010). MESSENGER observations of extreme loading and unloading of Mercury's magnetictail. *Science*, *329*(5992), 665–668. https://doi.org/10.1126/science.1188067

Slavin, J. A., Anderson, B. J., Baker, D. N., Benna, M., Boardsen, S. A., Gold, R. E., et al. (2012). MESSENGER and Mariner 10 flyby observations of magnetotail structure and dynamics at Mercury. *Journal of Geophysical Research*, *117*, A01215.

Slavin, J. A., Baker, D. N., Craven, J. D., Elphic, R. C., Fairfield, D. H., Frank, L. A., et al. (1989). CDAW 8 observations of plasmoid signatures in the geomagnetic tail: An assessment. *Journal of Geophysical Research*, *94*(A11), 15,153–15,175. https://doi.org/10.1029/JA094iA11p15153

Slavin, J. A., Lepping, R. P., Gjerloev, J., Fairfield, D. H., Hesse, M., Owen, C. J., et al. (2003). Geotail observations of magnetic flux ropes in the plasma sheet. *Journal of Geophysical Research*, *108*(A1), 1015. https://doi.org/10.1029/2002JA009557

Slavin, J. A., Owen, C. J., Kuznetsova, M. M., & Hesse, M. (1995). ISEE 3 observations of plasmoids with flux rope magnectic topologies. *Geophysical Research Letters*, *22*(15), 2061–2064. https://doi.org/10.1029/95GL01977

Slavin, J. A., Smith, M. F., Mazur, E. L., Baker, D. N., Hones, E. W., Iyemori, T., & Greenstadt, E. W. (1993). ISEE 3 observations of traveling compression regions in the Earth's magnetotail. *Journal of Geophysical Research*, *98*(A9), 15,425–15,446. https://doi.org/10.1029/93JA01467

Sonnerup, B. U. Ö., & Cahill, L. J. Jr. (1967). Magnetopause structure and attitude from Explorer 12 observations. *Journal of Geophysical Research*, *72*(1), 171–183. https://doi.org/10.1029/JZ072i001p00171

Sonnerup, B. U. Ö., & Scheible, M. (1998). Minimum and maximum variance analysis. In G. Paschmann, & P. W. Daly (Eds.), *Analysis methods for multi-spacecraft data* (Chap. 8, pp. 185–220). Noordwijk: European Space Agency.

Spencer, J. R., Pearl, J. C., Segura, M., Flasar, F. M., Mamoutkine, A., Romani, P., et al. (2006). Cassini encounters Enceladus: Background and the discovery of a south polar hot spot. *Science*, *311*(5766), 1401–1405. https://doi.org/10.1126/science.1121661

Stone, E. C., & Miner, E. D. (1986). The Voyager 2 encounter with the Uranian system. *Science*, *233*(4759), 39–43. https://doi.org/10.1126/science.233.4759.39

Stone, E. C., & Miner, E. D. (1989). The Voyager 2 encounter with the Neptunian system. *Science*, *246*(4936), 1417–1421. https://doi.org/10.1126/science.246.4936.1417

Thomas, N., Bagenal, F., Hill, T. W., & Wilson, J. K. (2004) ch. 23). The Io neutral clouds and plasma torus, in Jupiter. In F. Bagenal, T. E. Dowling, & W. B. McKinnon (Eds.), *Jupiter: The planet, satellites and magnetosphere* (pp. 561–592). Cambridge: University Press.

Tóth, G., Kovács, D., Hansen, K. C., & Gombosi, T. I. (2004). Three-dimensional MHD simulations of the magnetosphere of Uranus. *Journal of Geophysical Research*, *109*(A11), A11210. https://doi.org/10.1029/2004JA010406

Vasyliunas, V. M. (1986). The convection-dominated magnetosphere of Uranus. *Geophysical Research Letters*, *13*(7), 621–623. https://doi.org/10.1029/GL013i007p00621

Vogt, M. F., Jackman, C. M., Slavin, J. A., Bunce, E. J., Cowley, S. W. H., Kivelson, M. G., & Khurana, K. K. (2014). Structure and statistical properties of plasmoids in Jupiter's magnetotail. *Journal of Geophysical Research: Space Physics*, *119*, 821–843.

Vogt, M. F., Kivelson, M. G., Khurana, K. K., Joy, S. P., & Walker, R. J. (2010). Reconnection and flows in the Jovian magnetotail as inferred from magnetometer observations. *Journal of Geophysical Research*, *115*, A06219.

Voigt, G.-H., Behannon, K. W., & Ness, N. F. (1987). Magnetic field and current structures in the magnetosphere of Uranus. *Journal of Geophysical Research*, *92*(A13), 15,337–15,346. https://doi.org/10.1029/JA092iA13p15337